

ENCLOSURE 3 TO AEP-NRC-2014-59

**Babcock & Wilcox Report, S-1473-002, Revision 0, "Examination of Clevis Bolts Removed from
D. C. Cook Nuclear Plant"**




FINAL REPORT:

**EXAMINATION OF CLEVIS BOLTS REMOVED
FROM D. C. COOK NUCLEAR PLANT**

Prepared by:

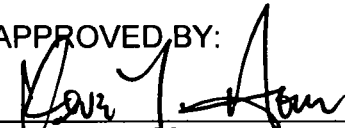
Babcock & Wilcox Technical Services Group
2016 Mount Athos Road
Lynchburg, Virginia 24504-5447
(434) 522-6000

PREPARED BY:



J. W. Hyres, P. E., Senior Principal Engineer
Nuclear Materials Engineering

APPROVED BY:



K. V. Hour, Manager
Nuclear Material & Inspection Services

SUMMARY

This report covers laboratory examinations performed by Babcock & Wilcox Technical Services Group (B&W TSG) on failed clevis bolts removed from the Lower Radial Support System (LRSS) at D. C. Cook Unit 1. Sixteen (16) broken bolts and thirteen (13) intact bolts (based on the post-removal visual inspections) were provided for laboratory analysis to evaluate the degradation, identify the failure mechanism(s), characterize the bolt material, and to evaluate the integrity of the intact bolts. The laboratory work scope included visual and stereovisual examinations of all bolts. Based on the results of these examinations, four bolts (two broken, two intact) were selected for more detailed analysis/testing, including scanning electron microscopy (SEM), energy dispersive spectroscopy (EDS), optical metallography, microhardness, chemical analysis by inductively coupled plasma-mass spectroscopy (ICP-MS), Rockwell hardness testing, and tensile testing.

All of the submitted bolts, including those considered to be intact, contained cracking in the head-to-shank transition. No cracking was identified in the threaded region of any of the bolts. There was a generally uniform open crack fracture pattern consisting of crack initiation at two diametrically opposing sides of the bolt in the head-to-shank transition and crack growth that extended upward into the bolt head at a $\sim 35^\circ$ angle relative to the bolt seating surface. The head separated from the shank when the two opposing cracks linked up near the center of the bolt cross section.

For each bolt, crack growth occurred along an axis of symmetry created by the opposing directions of crack growth. These crack growth axes indicated the direction of prevailing stresses in each bolt. No correlation between the orientations of the crack growth axes and the in-service orientations of the bolts within each clevis was observed. Minor differences in crack morphology around the circumference of the head-to-shank transition suggested that the magnitude of the prevailing stresses varied from bolt to bolt.

Fractographic SEM analysis and cross section metallographic examinations determined the fracture mode was essentially 100% intergranular with crack branching for all of the bolts.

The chemical analysis results for all four bolts were consistent with Alloy X-750 material. The mechanical properties and microstructure of the bolts were consistent with those published for Alloy X-750. No unexpected characteristics in the material properties, microstructures, or form of the bolts were identified.

The laboratory data indicated the bolts failed by intergranular stress corrosion cracking (IGSCC). The reported heat treatment for the bolts included a low solution annealing temperature and two-step aging treatment. Alloy X-750 material heat treated in this manner is known to have poor SCC cracking resistance in both high and low temperature water. There was no evidence that the bolts failed due to fatigue cracking or mechanical overload.

TABLE OF CONTENTS

<u>SECTION</u>	<u>PAGE</u>
LIST OF TABLES	iv
LIST OF FIGURES	v
LIST OF ACRONYMS.....	x
1.0 INTRODUCTION.....	1
2.0 BACKGROUND	1
3.0 RECEIPT VISUAL EXAMINATIONS.....	3
4.0 BOLT SELECTION	6
5.0 VISUAL/STEREOVISUAL INSPECTIONS.....	7
6.0 SECTIONING.....	8
7.0 SEM/EDS EXAMINATIONS.....	10
8.0 METALLOGRAPHIC EXAMINATIONS	12
9.0 VICKERS MICROHARDNESS.....	15
10.0 INDUCTIVELY COUPLED PLASMA-MASS SPECTROSCOPY (ICP-MS).....	17
11.0 ROCKWELL HARDNESS TESTING.....	18
12.0 TENSILE TESTING.....	18
13.0 ANALYSIS OF HEAD-TO-SHANK TRANSITION	20
14.0 DISCUSSION.....	21
15.0 CONCLUSIONS.....	24
16.0 REFERENCES.....	25

LIST OF TABLES

<u>TABLE</u>		<u>PAGE</u>
1	Summary of submitted bolts.....	1
2	Typical mechanical properties for Alloy X-750.	2
3	Visual examination summary of the bolts.....	3
4	Summary of bolts selected for destructive examinations.	6
5	Bolt 300°-1 head thickness measurements.....	9
6	Summary of Vickers microhardness (HV) results for bolt 120°-2 cross section.	15
7	Summary of Vickers microhardness (HV) results for bolt 120°-6 cross section.	15
8	Summary of Vickers microhardness (HV) results for bolt 240°-7 cross section.	16
9	Summary of Vickers microhardness (HV) results for bolt 300°-1 cross section	16
10	Summary of ICP-MS data.	17
11	Rockwell C hardness measurements.....	18
12	Summary of tensile test data.....	19

LIST OF FIGURES

<u>FIGURE</u>	<u>PAGE</u>
1	Schematic diagram showing the six clevis locations around the vessel circumference.26
2	Schematic showing the typical bolt configuration for each clevis insert.....26
3	Bolt 120°-2, annotated with laboratory rotational orientations.27
4	Bolt 120°-6, annotated with laboratory rotational orientations.27
5	Bolt 240°-7, annotated with laboratory rotational orientations.28
6	Bolt 300°-1, annotated with laboratory rotational orientations.28
7	Receipt macro photograph for bolt 0°-1.....29
8	Receipt macro photograph for bolt 0°-3.....29
9	Receipt macro photographs for bolt 0°-5.....30
10	Receipt macro photograph for bolt 0°-7.....31
11	Receipt macro photograph for bolt 60°-1.....31
12	Receipt macro photograph for bolt 60°-3.....32
13	Receipt macro photograph for bolt 60°-5.....32
14	Receipt macro photograph for bolt 60°-7.....33
15	Receipt macro photographs for bolt 120°-1.....34
16	Receipt macro photographs for bolt 120°-2.....35
17	Receipt macro photographs for bolt 120°-3.....36
18	Receipt macro photographs for bolt 120°-4.....37
19	Receipt macro photographs for bolt 120°-5.....38
20	Receipt macro photographs for bolt 120°-6.....39
21	Receipt macro photograph for bolt 120°-7.40
22	Receipt macro photographs for bolt 120°-8.....41
23	Receipt macro photographs for bolt 180°-1.....42
24	Receipt macro photograph for bolt 180°-3.....43
25	Receipt macro photographs for bolt 180°-7.....44
26	Receipt macro photographs for bolt 180°-8.....45
27	Receipt macro photograph for bolt 240°-1.....46
28	Receipt macro photograph for bolt 240°-3.....46
29	Receipt macro photograph for bolt 240°-5.....47

LIST OF FIGURES (CONTINUED)

<u>FIGURE</u>	<u>PAGE</u>
30	Receipt macro photograph for bolt 240°-7.....47
31	Receipt macro photograph for bolt 300°-1.....48
32	Receipt macro photographs for bolt 300°-3.....49
33	Receipt macro photographs for bolt 300°-5.....50
34	Receipt macro photographs for bolt 300°-6.....51
35	Receipt macro photographs for bolt 300°-7.....52
36	Receipt macro photographs for bolts from the 120° clevis.53
37	Receipt macro photographs for bolts 7 and 8 from the 180° clevis.55
38	Receipt macro photographs for bolts 5, 6, and 7 from the 300° clevis.56
39	Macro and stereo photographs of bolt 120°-2 taken at 45° increments.....57
40	Macro and stereo photographs of bolt 120°-6 taken at 45° increments.....61
41	Macro and stereo photographs of bolt 240°-7 taken at 45° increments.....65
42	Macro and stereo photographs of bolt 300°-1 taken at 45° increments.....69
43	Photograph showing wire EDM used to section each bolt for destructive examinations.73
44	Section photograph for bolt 240°-7 showing the typical locations chosen for subsequent analysis73
45	Typical location of tensile specimens machined from each bolt.74
46	Miniature tensile specimen design showing dimensions.74
47	Bolt 240°-7 after breaking open the crack for SEM/EDS75
48	Bolt 300°-1 showing plunge cut EDM surface, which removed much of the in-service cracking.....75
49	Macro photograph showing the open crack surface for bolt 120°-2.76
50	OD of 120°-2 near 90°, 50X77
51	Center of Figure 50, 500X77
52	Mid-diameter of 120°-2, 50X.....78
53	Center of Figure 52, 500X78
54	Center of 120°-2 fracture, 50X.....79
55	Center of Figure 54, 500X79
56	Macro photograph showing the open crack surface for bolt 120°-6.....80

LIST OF FIGURES (CONTINUED)

<u>FIGURE</u>	<u>PAGE</u>
57 OD of bolt 120°-6 near 45°, 50X.....	81
58 Center of Figure 57, 500X	81
59 Mid-diameter of bolt 120°-6, 50X.....	82
60 Center of Figure 59, 500X	82
61 Center of 120°-6 fracture, 50X.....	83
62 Center of Figure 61, 500X	83
63 Stereo microscope photograph showing the open crack surface for bolt 240°-7.....	84
64 OD of bolt 240°-7 near 315°, 50X.....	85
65 Center of Figure 64, 500X	85
66 Mid-diameter of 240°-7, 50X.....	86
67 Center of Figure 66, 500X	86
68 Center of 240°-7 fracture, 50X.....	87
69 Center of Figure 68, 500X	87
70 BSE image of titanium nitride ~15 µm in size, 1,500X.....	88
71 EDS spectrum collected from precipitate shown in Figure 70.	88
72 BSE image of niobium-titanium intermetallic ~20 µm long, 1,500X	89
73 EDS spectrum collected from precipitate shown in Figure 72.	89
74 Typical area of polished cross section, 1,500X	90
75 EDS spectrum collected from entire area shown in Figure 74.....	90
76 EDS dot maps collected from area shown in Figure 74.....	91
77 Tensile fracture surface for 240°-7L4, 80X.....	92
78 Same as Figure 77 with annotated reduction in area measurements, 80X	92
79 As-polished overview of bolt 120°-2 cross section. 6X	93
80 Same area as Figure 79 after phosphoric + nital etch. Structure is banded. 6X...	93
81 As-polished micrograph montage of crack. ~10X.....	94
82 Higher magnification detail of Figure 81, as-polished. 140X.....	95
83 Detail of initiation near 90°. 180X	96
84 Same area as Figure 83 above after phosphoric + nital etch. 180X.....	96
85 Detail of initiation near 270°. 180X	97

LIST OF FIGURES (CONTINUED)

<u>FIGURE</u>	<u>PAGE</u>
86	Same area as Figure 85 after phosphoric + nital etch. 180X.....97
87	Typical microstructure after phosphoric etch, DIC, 660X.....98
88	Same area as Figure 87 after phosphoric + nital etch, DIC, 660X.....98
89	Bolt 120°-6 cross section as-polished overview. 6X99
90	Same area as Figure 89 after phosphoric + nital etch. 6X.....99
91	As-polished micrograph montage of crack. ~10X..... 100
92	Higher magnification detail of Figure 91, as-polished. 140X..... 101
93	Detail of initiation near 45°. 180X 102
94	Same area as Figure 93 after phosphoric + nital etch. 180X..... 102
95	Detail of initiation near 225°. 180X 103
96	Same area as Figure 95 after phosphoric + nital etch. 180X..... 103
97	Typical microstructure after phosphoric etch, DIC, 660X..... 104
98	Same area as Figure 97 after phosphoric + nital etch, DIC, 660X..... 104
99	As-polished overview of 240°-7 cross section. 6X..... 105
100	Same area as Figure 99 after phosphoric + nital etch. 6X..... 105
101	As-polished micrograph montage of crack. 10X 106
102	Higher magnification detail of Figure 101, as-polished. 120X..... 107
103	Detail of initiation near 315° after etching. 180X..... 108
104	Second crack near 315°after etching. 180X 108
105	Detail of initiation near 135° after etching. 180X..... 109
106	Typical appearance of intermittent duplex grain structure, DIC. 90X..... 109
107	Typical microstructure after phosphoric etch, DIC, 660X..... 110
108	Same area as Figure 107 after phosphoric + nital etch, DIC, 660X..... 110
109	As-polished overview of 300°-1 cross section. 6X..... 111
110	Same area as Figure 109 after phosphoric + nital etch. 6X..... 111
111	Detail of initiation near 90°. 180X 112
112	Same area as Figure 111 after etching. 180X..... 113
113	Detail of initiation near 270°. 180X 114
114	Same area as Figure 113 after etching. 180X..... 114
115	Typical microstructure after phosphoric etch, DIC, 660X..... 115

LIST OF FIGURES (CONTINUED)

<u>FIGURE</u>	<u>PAGE</u>
116	Same area as Figure 115 after phosphoric + nital etch, DIC, 660X..... 115
117	Photograph showing the microhardness locations for 120°-2..... 116
118	Photograph showing the microhardness locations for 120°-6..... 116
119	Photograph showing the microhardness locations for 240°-7..... 117
120	Photograph showing the microhardness locations for 300°-1..... 117
121	Bolt 240°-7 at 135°. Circle radius is 0.065". 20X 118
122	Bolt 240°-7 at 315°. Circle radius is 0.065". 20X 118
123	Bolt 300°-1 at 90°. Circle radius is 0.069". 20X 119
124	Bolt 300°-1 at 270°. Circle radius is 0.069". 20X 119
125	Higher magnification montage of bolt 240°-7 at 135°. As-polished, ~70X 120
126	Higher magnification montage of bolt 240°-7 at 315°. As-polished, ~65X 121
127	Higher magnification montage of bolt 300°-1 at 90°. As-polished, ~80X 122
128	Higher magnification montage of bolt 300°-1 at 270°. As-polished, ~75X 123

LIST OF ACRONYMS

ASME.....	AMERICAN SOCIETY OF MECHANICAL ENGINEERS
ASTM.....	AMERICAN SOCIETY FOR TESTING AND MATERIALS
B&W TSG	BABCOCK & WILCOX TECHNICAL SERVICES GROUP
BSE.....	BACKSCATTERED ELECTRON (SEM IMAGING)
CW.....	CLOCKWISE
CCW	COUNTERCLOCKWISE
DIC.....	DIFFERENTIAL INTERFERENCE CONTRAST (OPTICAL IMAGING)
EDM.....	ELECTRICAL DISCHARGE MACHINING
EDS	ENERGY DISPERSIVE SPECTROSCOPY
HRC	ROCKWELL C HARDNESS (MACRO HARDNESS)
HTSCC	HIGH TEMPERATURE STRESS CORROSION CRACKING
HV.....	VICKERS HARDNESS (MICROHARDNESS)
ICP-MS	INDUCTIVELY COUPLED PLASMA-MASS SPECTROSCOPY
IGSCC	INTERGRANULAR STRESS CORROSION CRACKING
LRSS	LOWER RADIAL SUPPORT SYSTEM
LTCP.....	LOW TEMPERATURE CRACK PROPAGATION
OD	OUTER DIAMETER
OES	OPTICAL EMISSION SPECTROSCOPY
PWR	PRESSURIZED WATER REACTOR
RA.....	REDUCTION IN AREA
SCC	STRESS CORROSION CRACKING
SE	SECONDARY ELECTRON (SEM IMAGING)
SEM	SCANNING ELECTRON MICROSCOPE/MICROSCOPY

1.0 INTRODUCTION

This report covers laboratory examinations performed by Babcock & Wilcox Technical Services Group (B&W TSG) on failed clevis bolts removed from the Lower Radial Support System (LRSS) at D. C. Cook Unit 1.

Sixteen (16) broken bolts and thirteen (13) intact bolts were shipped to the B&W Lynchburg Technology Center for laboratory analysis to evaluate the degradation, identify the failure mechanism(s), characterize the bolt material, and to evaluate the integrity of the intact bolts. A summary of the submitted bolt samples (locations per Figure 1 and Figure 2) is provided in the table below:

Table 1: Summary of submitted bolts.

Location	Broken Bolt Locations	Intact Bolt Locations
0°	#5	#1, #3, #7
60°	---	#1, #3, #5, #7
120°	#1 through #8	---
180°	#1, #7, #8	#3
240°	---	#1, #3, #5, #7
300°	#3, #5, #6, #7	#1
Totals	16	13

The laboratory work scope included visual and stereovisual examinations, scanning electron microscopy (SEM), energy dispersive spectroscopy (EDS), optical metallography, Vickers microhardness, chemical analysis by inductively coupled plasma-mass spectroscopy (ICP-MS), Rockwell hardness testing and tensile testing. The goal of these examinations was to determine the most likely cause of the bolt failures.

2.0 BACKGROUND

Seven clevis bolts and one dowel pin in the LRSS had visual indications during the March 2010 refueling outage at D. C. Cook Unit 1. AEP replaced a minimum bolt pattern that encompassed all bolts with visual indications during the March/April 2013 refueling outage and it was determined that a total of 16 bolts had failed. In each case, the failure location was below the head in the head-to-shank transition.

The lower radial support system consists of six (6) support clevises spaced evenly around the reactor vessel circumference as shown schematically in Figure 1. Each clevis is comprised of a wear plate (insert) attached to the lugs by eight (8) bolts and two (2) press fit dowel pins (Figure 2). In all, there are 48 clevis bolts and 12 dowel pins in the lower radial support system.

The clevis bolts are approximately 3" long by 0.75" in diameter and are manufactured from Alloy X-750. The clevis bolt head is approximately 1.5" in diameter with a slotted internal hex socket to accommodate a locking bar. The locking bar is welded in place after installation to prevent backing out during operation. The on-site inspections indicated some of the locking bars were worn due to contact with the clevis bolt head. Inspection photos of the four bolts selected for detailed destructive analyses are presented in Figure 3 through Figure 6.

The clevis bolts were heat treated using a two-step aging treatment that consisted of:

- Hot roll
- Equalize (solution anneal) for 24 hours at 1625°F (885C) and air cool
- Solution anneal at 1775°F (968C) for one hour and air cool
- Age at 1,350°F (732C) for 8 hours
- Furnace cool to 1,150°F (621C) and age for 8 hours
- Air cool

This exact heat treatment was not found in any of the Alloy X-750 material specifications. Elements of this heat treatment are common to condition AH and condition BH, except that these heat treatments specify a single aging treatment at 1,300°F (704C) for 20 hours in lieu of the two-step aging treatment. Other two-step aging processes, such as ASME Code Case N-60-5, SB-637, Grade 688, Type 2, employ a higher solution annealing temperature, 1,800°F (982C) along with the same two-step process described above (Ref. 1).

Mechanical properties for each of these heat treatments are summarized in the table below:

Table 2: Typical mechanical properties for Alloy X-750.

Condition	UTS, ksi	YS, ksi	% Elong.	RA, %
AH	173 typ.	119 typ.	26 typ.	44 typ.
BH	198 typ.	145 typ.	22 typ.	41 typ.
SB-637, Type 2	170 min.	115 min.	18 min.	18 min.

It can be seen that the ultimate strength and yield strength values are significantly higher for condition BH compared to condition AH. The higher strength of condition BH is offset by lower elongation and reduction in area (RA) values compared to condition AH. The condition AH and SB-637, Type 2 strength levels are comparable.

3.0 RECEIPT VISUAL EXAMINATIONS

Macro photographs were taken of the intact bolts and bolt fragments to document their as-received condition. The bolt fragments (i.e. head and shank) were photographed separately; the intact bolts were photographed in the head-to-shank transition region.

Detailed visual inspections were then performed on the as-received bolts and fragments under the stereomicroscope at magnifications up to 50X. These inspections were used to assess the overall condition of the bolts/fragments and help select candidate bolts for the destructive examinations. The results of these inspections are detailed in the following table. The four bolts selected for detailed examinations are shown in **bold**.

Table 3: Visual examination summary of the bolts.

<i>In-Service Location*</i>	<i>Shipping ID</i>	<i>Report Figure</i>	<i>Broken/Intact</i>	<i>Rubbed Fracture?</i>	<i>Typical Pattern?</i>	<i>Additional Comments</i>
0°-1	A-1	7	Intact	N/A	Yes	Most angled cracking at this clevis location.
0°-3	A-8	8	Intact	N/A	Yes	Less angled cracking than 0°-1
0°-5	A-10	9	Broken	N/A	N/A	<i>Fracture surface lost due to EDM plunge cut.</i>
0°-7	A-9	10	Intact	N/A	Yes	Least angled cracking at this clevis location.
60°-1	B-1	11	Intact	N/A	Yes	Most angled cracking at this clevis location.
60°-3	B-13	12	Intact	N/A	Yes	Less angled cracking compared to 60°-1.
60°-5	B-4	13	Intact	N/A	Yes	Cracking tighter and not 360° around.
60°-7	B-14	14	Intact	N/A	Yes	Less angled cracking compared to 60°-1.
120°-1	B-15	15	Broken	Yes	Yes	Angled cracking present around OD.
120°-2	B-12	16	Broken	No	Yes	Less angled cracking compared to 120°-1 or 120°-4.
120°-3	B-5	17	Broken	Yes	Yes	Less angled cracking compared to 120°-1 or 120°-4.
120°-4	B-3	18	Broken	Yes	Yes	Angled cracking present around OD.

*In-service location consists of the angular orientation of the clevis (0°, 60°, 120°, etc.) along with the bolt position (1, 2, 3, etc.). Refer to Figure 1 and Figure 2.

Table 3 (continued): Visual examination summary of the bolts.

<i>In-Service Location*</i>	<i>Shipping ID</i>	<i>Report Figure</i>	<i>Broken/Intact</i>	<i>Rubbed Fracture?</i>	<i>Typical Pattern?</i>	<i>Additional Comments</i>
120°-5	B-2	19	Broken	Yes	Yes	Angled cracking present around OD.
120°-6	B-16	20	Broken	No	No	Very minor angled cracking around OD.
120°-7	B-6	21	Broken	N/A	N/A	Fracture surface lost due to EDM plunge cut.
120°-8	B-11	22	Broken	Yes	Yes	Angled cracking present around OD.
180°-1	A-12	23	Broken	N/A	N/A	Fracture surface lost due to EDM plunge cut.
180°-3	A-3	24	Intact	N/A	Yes	Minor angled cracking around OD.
180°-7	A-14	25	Broken	Yes	Yes	Less angled cracking compared to 180°-8; asymmetric center.
180°-8	A-13	26	Broken	Yes	Yes	Most angled cracking at this clevis location; asymmetric center.
240°-1	A-16	27	Intact	N/A	Yes	Less angled cracking compared to 240°-7.
240°-3	A-15	28	Intact	N/A	Yes	Less angled cracking compared to 240°-5.
240°-5	A-4	29	Intact	N/A	Yes	Less angled cracking compared to 240°-1.
240°-7	A-6	30	Intact	N/A	Yes	Most angled cracking at this clevis location.
300°-1	A-7	31	Intact	N/A	No	Very minor angled cracking around OD.
300°-3	A-2	32	Broken	N/A	N/A	Fracture surface lost due to EDM plunge cut.
300°-5	B-9	33	Broken	Yes	Yes	Less angled cracking compared to 300°-7.
300°-6	B-10	34	Broken	Yes	Yes	Most angled cracking at this clevis location.
300°-7	B-8	35	Broken	Yes	Yes	Less angled cracking compared to 300°-6.

*In-service location consists of the angular orientation of the clevis (0°, 60°, 120°, etc.) along with the bolt position (1, 2, 3, etc.). Refer to Figure 1 and Figure 2.

It was determined that the fracture surfaces on four of the broken bolts (0°-5, 120°-7, 180°-1, and 300°-3) were destroyed during removal due to EDM plunge cutting. These four bolts (shown in *italics* in Table 3) were not examined further.

Macro photographs were taken of the twelve (12) open fracture surfaces using side lighting to highlight the fracture surface texture. The bolt photographs are presented in Figure 36 (120° clevis), Figure 37 (180° clevis), and Figure 38 (300° clevis). In these figures, the bolts are arranged by their position within the clevis. Also, the orientation of each bolt was matched to the in-service orientation, i.e. the 12:00 position in the photograph matches the 12:00 in-service position.

Many of the open fractures sustained considerable rubbing damage and were not considered good candidates for the higher magnification examinations. However, it was evident that all of the open fracture surfaces followed a similar pattern. Crack growth progressed inward from the head/shank transition at a ~35° angle relative to horizontal toward the center of the bolt from two diametrically opposed sides. The axis of symmetry created by these two opposing sides is annotated on each fracture surface in Figure 36 through Figure 38. The orientations of the axes of symmetry were random in nature, which indicated the directions of prevailing stresses were variable within each clevis and between different clevises. Final fracture occurred when the two opposing cracks linked together near the center of the bolt.

All of the thirteen (13) intact bolts contained cracking in the head/shank transition. No cracking was identified in the threaded region of any bolt. Most of the intact bolts exhibited a common cracking pattern consisting of a straight, unbranched crack for approximately half of the circumference, while the other half had many angular cracks that may or may not have linked up. Broken bolts exhibited a similar pattern when observing crack elevation variations around the bolt OD in the head to shank transition.

The amount of angled cracking varied somewhat among the bolts, from many angled cracks (e.g. 240°-7) to very few angled cracks (e.g. 300°-1). The amount of angled cracking is expected to decrease as the stress increases, but this variation in crack morphology could also indicate a failure mode change.

4.0 BOLT SELECTION

It was decided to select two intact and two broken bolts for the destructive examinations. It was also important to select bolts that exhibited a higher degree of angled cracking and bolts with little or no angled cracking. Of secondary concern was capturing bolts from the different clevis orientations and from different positions within a particular clevis (i.e. high/low, left/right).

It was determined that the following bolts would be subjected to the destructive examinations: 120°-2, 120°-6, 240°-7, and 300°-1. The goal of the selection process was to capture as many variables as possible within the limits of the authorized work scope.

A summary of the selected bolts is provided in the table below:

Table 4: Summary of bolts selected for destructive examinations.

Bolt ID	Broken/Intact	Fits Typical Pattern?	Left/Right	High/Low
120-2	Broken	Yes	Left	High
120-6	Broken	No	Right	High
240-7	Intact	Yes	Right	Low
300-1	Intact	No	Left	High

The selected bolts were located in three of the six clevis locations and included two bolts from the 120° clevis. The 120° clevis location experienced the greatest population of in-service bolt failures (all 8 bolts failed).

5.0 VISUAL/STEREOVISUAL INSPECTIONS

Detailed visual and stereovisual inspections were performed on the four selected bolts. Photographs were taken at 45° increments to document the extent and nature of the cracking. The angular orientations were established by assigning the 0° position to the 12:00 in-service position and increasing degrees in the clockwise direction when viewing the bolt head.

Bolt 120°-2

The macro and stereo photographs for bolt 120°-2 are presented in Figure 39. The fracture surface was dark brown in color and exhibited some branching around the circumference. The fracture surface axis of symmetry was in the 90°-270° direction.

Bolt 120°-6

The macro and stereo photographs for bolt 120°-6 are presented in Figure 40. The fracture surface was lighter in color than bolt 120°-2, which suggested less surface deposits were present and this fracture likely occurred more recently than the 120°-2 bolt failure. Cracking was generally straight and exhibited very minor branching around the circumference. The fracture surface axis of symmetry was in the 45°-225° direction.

Bolt 240°-7

The macro and stereo photographs for bolt 240°-7 are presented in Figure 41. Crack branching is evident around nearly the entire circumference with the exception of the 315° orientation (i.e. 10:30 in-service).

Bolt 300°-1

The macro and stereo photographs for bolt 300°-1 are presented in Figure 42. Cracking was generally straight and exhibited very minor branching around the circumference.

6.0 SECTIONING

Sectioning was required to permit the higher magnification metallographic and SEM examinations of the bolt fractures, as well as chemical analysis and mechanical testing of the bolt material. The sectioning was accomplished using wire electrical discharge machining (EDM).

Hardness, Tensile, and Chemical Analysis Specimens

The hardness and tensile specimens were machined from the threaded portion of each bolt. To produce these specimens, a rectangular bar measuring 0.5" x 0.5" x 2.2" was machined from the threaded region as shown in Figure 43. One surface of each bar was then ground for Rockwell C hardness measurements. The location of these measurements for bolt 240°-7 is shown in Figure 44. The hardness measurement locations were typical for all four bolts. Also shown in Figure 44 is the typical location of the disk-shaped chemical analysis specimen, which was machined from the unthreaded portion of each bolt shank.

After the hardness testing was complete, the tensile specimens were profiled out of the rectangular bar as shown in Figure 45. At least 0.030" of material was machined from the hardness testing surface to ensure the tensile specimens were not influenced by localized cold working introduced during hardness testing. In all, 20 tensile specimens were machined from each bolt, 10 "upper" specimens from near the head (identified as U1 through U10) and 10 "lower" specimens away from the head (identified as L1 through L10).

The miniature tensile specimen dimensions are provided in Figure 46. This design was selected because it is consistent with ASTM E 8 (Ref. 2), and owing to its smaller size, permits testing of several specimens from a relatively small amount of material.

Open Crack SEM and Cross Section Metallographic Specimens

The open crack SEM examinations were performed on the head side of each fracture surface. For the broken bolts, 120°-2 and 120°-6, the entire fracture surface was examined. For the intact bolt, 240°-7, the bolt head was first split through the 135°-315° orientation to produce specimens for open crack SEM and cross section metallography. Figure 47 shows the mating halves of the fracture surface of bolt 240°-7 after breaking open the crack. It was estimated that the crack opened with just a few pounds of force, i.e. there was a very small amount of remaining ligament as evidenced by the lack of shiny laboratory fracture on the open crack surfaces.

It was necessary to reduce the thickness of the three open crack specimens to facilitate the SEM examinations. Care was taken to ensure the bottom of the hex and the fracture surface were not damaged during cutting. The location of this cut for bolt 240°-7 is shown in Figure 44. The broken bolt heads from bolt 120°-2 and bolt 120°-6 were cut in a similar manner.

After the SEM examinations were completed on the two broken bolt heads, the fracture surfaces were sectioned through their axis of symmetry for the cross section metallography examinations.

The 300°-1 bolt was plunge EDM cut during removal from service, which eliminated most of the in-service cracking (Figure 48). Measurements of the EDM plunge cut depth indicated only ~0.020" of the cracking remained for examination. In order to capture the maximum extent of the remaining crack, thickness measurements were taken around the head circumference as shown in the table below:

Table 5: Bolt 300°-1 head thickness measurements.

Orientation	Thickness, in.
0°	0.242
90°	0.253
135°	0.250
180°	0.244
270°	0.231
315°	0.236

These measurements indicated the EDM plunge cutter was located slightly toward the 270° orientation (i.e. minimum thickness value). The 90°-270° orientation was selected for the cross section metallographic examinations to provide the highest probability of capturing the longest remaining crack length, which was expected to be at the 90° orientation.

Since relatively little cracking was present in bolt 300°-1, it was decided to perform the SEM examinations on a polished cross section prepared from the threaded region rather than an open crack specimen. The cross section analysis would provide an opportunity to examine the microstructure at higher magnifications and perform EDS chemical analysis to characterize the bulk material and precipitates.

7.0 SEM/EDS EXAMINATIONS

Fracture surfaces and polished metallographic cross sections of the four bolts were examined by SEM equipped with EDS for elemental analysis. Both secondary electron (SE) and backscattered electron (BSE) imaging modes were utilized to characterize the bolts. SE imaging was used to document the fracture surface morphology, while BSE imaging (identified as AUX1 in Figures 70, 72, and 74) was used to characterize the material microstructure on the cross sections. The fractographic examinations were performed on bolts 120°-2, 120°-6, and 240°-7. The microstructural characterizations were performed on an as-polished cross section prepared from the threaded region of bolt 300°-1.

Bolt 120°-2 Open Crack

A low magnification photograph showing the open crack from bolt 120°-2 is shown in Figure 49. Annotated on this figure are three areas selected for higher magnification examinations, which included the OD surface near 90° (Figure 50 and Figure 51), the mid-diameter (Figure 52 and Figure 53), and near the center of the fracture surface (Figure 54 and Figure 55). Cracking was essentially 100% intergranular fracture, with the exception of a small amount of mixed mode fracture near the center of the bolt fracture surface. This central area contained a mixture of intergranular fracture, transgranular cleavage, and a small amount of ductile fracture (Figure 55). Surface deposits were noted on the fracture surface. EDS analysis indicated these deposits were base metal oxides. The presence of these deposits was consistent with the relatively dark macro appearance of the fracture surface.

Bolt 120°-6 Open Crack

A low magnification photograph showing the open crack from bolt 120°-6 is shown in Figure 56. Annotated on this figure are three areas selected for higher magnification examinations, which included the OD surface near 45° (Figure 57 and Figure 58), the mid-diameter (Figure 59 and Figure 60), and near the center of the fracture surface (Figure 61 and Figure 62). Cracking was essentially 100% intergranular fracture. There was no evidence of mixed mode near the center as was the case for the 120°-2 bolt. Less surface oxides/deposits were present on this fracture surface. This is consistent with the macro appearance of the fractures, i.e. bolt 120°-6 appeared "cleaner" than bolt 120°-2.

Bolt 240°-7 Open Crack

A low magnification photograph showing the open crack from bolt 240°-7 is shown in Figure 63. Annotated on this figure are three areas selected for higher magnification examinations, which included the OD surface near 315° (Figure 64 and Figure 65), the mid-diameter (Figure 66 and Figure 67), and near the center of the fracture surface (Figure 68 and Figure 69). The fracture mode was essentially 100% intergranular.

Bolt 300°-1 Mounted Cross Section

A polished cross section prepared through the threaded portion of bolt 300°-1 was analyzed by SEM/EDS. Typical precipitates identified during these examinations included titanium nitride measuring ~15 µm in size (Figure 70 and Figure 71) and niobium-titanium intermetallic measuring ~20 µm long by ~6 µm wide (Figure 72 and Figure 73). Carbon was not detected in any of the examined areas; therefore, specific carbide types ($M_{23}C_6$ vs. MC) could not be differentiated. Subsequent optical examinations described in Section 5.0 indicated the carbides were very fine (<1 µm) and smaller than the EDS analysis volume.

The typical microstructure for this material is shown in Figure 74. The standardless quantitation performed on this area is shown in Figure 75. The chemical analysis results were generally consistent with Alloy X-750 material.

High resolution EDS dot maps were also collected from this area and are presented in Figure 76. When interpreting these maps, note that the concentration of an element increases with increasing color density within that element's window, i.e. darker color indicates more of that element is present. The maps indicated the primary elements present were nickel, chromium, and iron; trace amounts of titanium and niobium were detected as well. The maps also show that the composition of the alloy base metal was uniform (no significant, widespread contrast in the maps) and that there was a higher concentration of niobium and titanium in the precipitates, as indicated by the discrete darker regions within the niobium and titanium element windows.

Tensile Fracture Surfaces

Low magnification (80X) SE imaging was used to document each tensile specimen fracture. Low magnification micrographs were taken of each surface in order to accurately measure the reduced section area, since standard techniques such as calipers can be problematic when measuring miniature specimens. A typical example of a tensile fracture is shown in Figure 77. The fracture surface was mixed mode that consisted of intergranular facets and ductile microvoid coalescence. The potential implications of this finding are discussed further in Section 13.0.

Thickness and width measurements were then made to determine the reduction in area for each specimen. Typical measurements are annotated on the micrograph as shown in Figure 78.

8.0 METALLOGRAPHIC EXAMINATIONS

Metallographic examinations were performed on the mounted cross section specimens prepared through cracking in the four bolts. The mounting material used was a long cure two-part epoxy compound. The mounts were analyzed first in the as-polished condition and after chemical etching to reveal the material microstructure.

The dual etch procedure was used on the bolt material. This procedure involves etching the polished cross section in concentrated phosphoric acid to reveal the carbides, then etching in 5% nital to reveal the material grain boundaries. Electrolytic etching (3V for 15 seconds) was used for both steps. The dual etch technique is frequently used to determine the carbide distribution (i.e. intergranular vs. intragranular) in Alloy 600. Differential interference contrast (DIC) lighting was used to evaluate the carbide distribution.

Bolt 120°-2 Cross Section

Low magnification stereo microscope photographs were taken of the bolt 120°-2 cross section in the as-polished (Figure 79) and etched (Figure 80) conditions. The banded nature of the microstructure was evident at low magnification in the etched condition. Crack propagation traversed the banded regions, an indication that cracking was not directly influenced by the presence of a banded microstructure.

A multi-frame montage of the entire crack is presented in Figure 81. A higher magnification montage showing the extent of cracking toward the bottom of the hex (top of montage) is presented in Figure 82. Cracking exhibited a branched intergranular morphology in all areas examined.

Higher magnification detail micrographs were also taken of each initiation region. The 90° micrographs are shown in Figure 83 and Figure 84. The 270° micrographs are shown in Figure 85 and Figure 86. Evidence of a second, shallower crack was noted at both locations, as was the banded microstructure. There was no obvious evidence of surface cold work at either initiation region.

Typical DIC micrographs showing the microstructure after phosphoric acid etching and nital etching are presented in Figure 87 and Figure 88, respectively. The carbides (fine black dots) were present in discrete bands, as evidenced by a vertical band on the left and right of the micrographs. The center region contained relatively few carbides. The carbides were typically intragranular; a slight amount of grain boundary carbide coverage was noted (<25%).

Bolt 120°-6 Cross Section

Low magnification stereo microscope photographs were taken of the bolt 120°-6 cross section in the as-polished (Figure 89) and etched (Figure 90) conditions. The banded nature of the microstructure was evident at low magnification. Crack propagation traversed the banded regions, an indication that cracking was not directly influenced by the presence of a banded microstructure.

A multi-frame montage of the entire crack is presented in Figure 91. A higher magnification montage showing the extent of cracking at the crack apex is presented in Figure 92. Cracking exhibited a branched intergranular morphology in all areas examined.

Higher magnification detail micrographs were also taken of each initiation region. The 45° micrographs are shown in Figure 93 and Figure 94. The 225° micrographs are shown in Figure 95 and Figure 96. Very little, if any, crack branching was noted at each initiation, which is consistent with the relative lack of angled cracking noted around the bolt OD. There was no obvious evidence of surface cold work at either initiation region.

Typical DIC micrographs showing the microstructure after phosphoric acid etching and nital etching are presented in Figure 97 and Figure 98, respectively. A discrete band of carbides (fine black dots) is visible toward the left side of the micrograph. Relatively few carbides were noted elsewhere. The carbides were typically intragranular; a slight amount of grain boundary carbide coverage was noted (<25%).

Bolt 240°-7 Cross Section

Low magnification stereo microscope photographs were taken of the bolt 240°-7 cross section in the as-polished (Figure 99) and etched (Figure 100) conditions. The banded nature of the microstructure was evident at low magnification. Crack propagation traversed the banded regions, an indication that cracking was not directly influenced by the presence of a banded microstructure.

A multi-frame montage of the entire crack is presented in Figure 101. A higher magnification montage showing the nature of the crack branching is presented in Figure 102. Two cracks were located at the 315° orientation, i.e. the cross section cut through two adjacent, overlapping cracks at this orientation. Cracking exhibited a branched intergranular morphology in all areas examined.

Higher magnification detail micrographs were also taken of each initiation region. The 315° micrographs are shown in Figure 103 and Figure 104. Two separate cracks were present at this location. The 135° micrograph is shown in Figure 105. There was no obvious evidence of surface cold work at either initiation region. A low magnification DIC micrograph showing the typical appearance of the duplex microstructure is presented in Figure 106. The microstructure was primarily comprised of fine, equiaxed grains (ASTM ~7-8) with some large, abnormal grains (ASTM ~1-2).

Typical DIC micrographs showing the microstructure after phosphoric acid etching and nital etching are presented in Figure 107 and Figure 108, respectively. A discrete carbide band (fine black dots) is visible toward the right side of the micrograph. A few carbides were noted on the left side of the micrograph. The carbides were typically intragranular; a slight amount of grain boundary carbide coverage was noted (<25%).

Bolt 300°-1 Cross Section

Low magnification stereo microscope photographs were taken of the bolt 300°-1 cross section in the as-polished (Figure 109) and etched (Figure 110) conditions. The banded nature of the microstructure was evident at low magnification. Crack propagation traversed the banded regions, an indication that cracking was not directly influenced by the presence of a banded microstructure. The EDM plunge cut depth is also indicated in Figure 109.

Higher magnification detail micrographs were taken of each initiation region. The 90° micrographs are shown in Figure 111 (as-polished) and Figure 112 (etched). The 270° micrographs are shown in Figure 113 (as-polished) and Figure 114 (etched). The available crack length was approximately 0.025" at 90° and 0.020" at 270°. Cracking was primarily intergranular, except for one instance where cracking was transgranular through a large grain at the 90° orientation (denoted by arrows in Figure 112). Minor secondary cracking was noted in this cross section and was mainly located adjacent to the plunge EDM surface (along the top edge of the micrographs). Crack branching was also minor and extended 1-2 grains deep from the main crack.

Typical DIC micrographs showing the microstructure after phosphoric acid etching and nital etching are presented in Figure 115 and Figure 116, respectively. A discrete carbide band (fine black dots) is visible toward the right side of the micrograph. Relatively few carbides were noted elsewhere. The carbides were typically intragranular; a slight amount of grain boundary carbide coverage was noted (~<25%).

9.0 VICKERS MICROHARDNESS

Several Vickers microhardness (HV) readings (500 gram load) were taken on the mounted specimens to characterize the hardness in various areas of interest, including near the OD in the initiation regions, mid-thickness, and bulk material away from the cracking. The areas selected are shown in Figure 117 through Figure 120. For the intact bolts, hardness measurements were taken both above and below the cracking.

The Vickers microhardness (HV) results are summarized in the tables below:

Table 6: Summary of Vickers microhardness (HV) results for bolt 120°-2 cross section.

Reading	Initiation 90°	Initiation 270°	Mid-Crack	Bulk 90°	Bulk 180°
#1	433	397	408	408	388
#2	338*	374	410	398	407
#3	413	377	445	413	412
#4	416	399	421	405	413
#5	398	416	429	400	407

*Reading disregarded due to edge effect (i.e. too close to edge of specimen).

Table 7: Summary of Vickers microhardness (HV) results for bolt 120°-6 cross section.

Reading	Initiation 315°	Initiation 135°	Mid-Crack	Bulk 315°	Bulk 135°
#1	396	397	400	399	405
#2	392	394	395	422	409
#3	380	358	365	400	396
#4	380	394	407	387	390
#6	392	393	387	405	395

Table 8: Summary of Vickers microhardness (HV) results for bolt 240°-7 cross section.

Reading	Initiation 135°	Initiation 315°	Mid-Crack	Bulk 135°	Bulk 315°
#1	389	408	407	412	426
#2	390	403	390	411	426
#3	371	394	396	413	404
#4	375	408	402	409	420
#5	401	403	392	393	414
#6	400	388	---	---	---
#7	391	384	---	---	---
#8	392	440	---	---	---
#9	386	390	---	---	---
#10	393	389	---	---	---

Note: Initiation readings #1-#5 were taken above the crack; readings #6-#10 were taken below the crack. Five readings were taken at the mid-crack, bulk 135°, and bulk 315° locations.

Table 9: Summary of Vickers microhardness (HV) results for bolt 300°-1 cross section.

Reading	Initiation 90°	Initiation 270°	Bulk 90°	Bulk 180°
#1	394	405	404	410
#2	412	402	434	415
#3	409	395	420	395
#4	402	415	432	406
#5	390	402	373	415

The results for the initiation regions and bulk material were generally consistent and as expected for Alloy X-750 material (~400 HV). The results were also consistent with the Rockwell C hardness values, refer to Section 11.0. There was no evidence of significant surface cold work near the initiation regions.

10.0 CHEMICAL ANALYSIS

Small pieces (~100mg each) were removed from each of the four candidate bolts and analyzed by Inductively Coupled Plasma - Mass Spectroscopy (ICP-MS) for base material constituents, including: nickel, chromium, iron, cobalt, niobium, titanium, aluminum, manganese, silicon, copper, sulfur, phosphorus, boron, zirconium, and vanadium. Note that this technique cannot determine carbon content. The results are summarized in the table below:

Table 10: Summary of ICP-MS Data.

Element	Alloy X-750	120°-2	120°-6	240°-7	300°-1
Nickel	70.0 min	71.8	73.0	72.8	72.4
Chromium	14.0 - 17.0	15.7	15.6	15.7	15.5
Iron	5.0 - 9.0	7.5	7.3	7.2	7.3
Titanium	2.25 - 2.75	2.32	2.10	2.13	2.46
Aluminum	0.4 - 1.0	0.87	0.82	0.81	0.80
Niobium + Tantalum	0.7 - 1.2	0.85	0.62	0.82	0.92
Manganese	1.0 max	0.20	0.12	0.12	0.12
Silicon	0.5 max	0.02	0.02	0.03	0.02
Sulfur	0.01 max	<0.003	<0.003	<0.003	<0.003
Copper	0.5 max	0.03	0.01	0.01	0.01
Carbon*	0.08 max	--	--	--	--
Cobalt	1.0 max	0.31	0.06	0.06	0.06
Phosphorus	--	0.006	0.003	0.006	0.005
Boron	--	0.004	0.004	0.004	0.004
Zirconium	--	0.05	0.07	0.08	0.08
Vanadium	--	0.26	0.26	0.24	0.27

*Not determined.

The niobium + tantalum and titanium concentrations were marginally low for the 120°-6 bolt and the titanium was marginally low for the 240°-7 bolt (bolded values in Table 10). However, the concentrations were considered to be consistent with Alloy X-750, when accounting for the uncertainty of the ICP-MS technique and the additional tolerance allowed by the material specification when performing product (also called "check") analysis (Ref. 3). This additional tolerance is provided to account for variations that may occur between components made from the same heat lot. For titanium, the product tolerance is 0.07% below the minimum, or 2.18%. For niobium + tantalum, the product tolerance is 0.05% below the minimum, or 0.65%.

It was noted that the trace element levels (manganese, cobalt, and copper) were higher in the 120°-2 bolt compared to the other three bolts. This indicated the 120°-2 bolt likely originated from a different heat lot.

Carbon concentration cannot be reliably determined using ICP-MS due to low ion efficiency. Techniques typically used to determine the carbon concentration in bulk metals include combustion and optical emission spectroscopy (OES). OES is also preferred over ICP-MS for determining bulk chemical analysis of metals. Unfortunately, no laboratories capable of performing OES on irradiated specimens were identified during the course of this examination.

11.0 ROCKWELL HARDNESS MEASUREMENTS

Rockwell C hardness measurements (diamond indenter, 150 kg load) were taken to determine the bolt material bulk hardness. These measurements were taken on the tensile specimen blank removed from each of the four candidate bolts. Figure 44 shows the typical location of the five (5) hardness measurements taken on each tensile blank. The EDM recast layer was ground off prior to performing the hardness measurements. The results are summarized below:

Table 11: Rockwell C hardness measurements.

Reading	120°-2	120°-6	240°-7	300°-1
#1	39.4	38.8	38.7	39.0
#2	39.0	38.9	38.7	39.0
#3	39.1	38.9	39.0	38.8
#4	38.9	39.1	39.1	39.0
#5	39.1	39.2	39.0	39.1
Average	39.1	39.0	38.9	39.0

The results were very consistent for each bolt and between the four bolts and were as expected for Alloy X-750 material. The ASTM A 370 (Ref. 4) conversion for HRC 39 is 177 ksi UTS, which is generally consistent with the tensile testing results, refer to Section 12.0.

12.0 TENSILE TESTING

Tensile testing was performed in accordance with B&W Technical Procedure TP-78, "Tension Testing of Metallic Materials" (Ref. 5). This specification is consistent with ASTM E8 (Ref. 2). These tests were used to determine the bolt material yield strength, ultimate tensile strength, percent elongation, and reduction in area. Figure 3.5 shows the miniature tensile specimen geometry, which was consistent with ASTM E8, except on a miniature scale to increase the number of samples tested per bolt.

Eight tensile specimens were tested from each bolt, including the #1, #4, #7, and #10 "upper" specimens located closer to the bolt head and the #1, #4, #7, and #10 "lower" specimens located away from the head. The tensile test data was very consistent for the #1, #4, and #7 samples. All of these specimens broke in the center of the gage length. However, the #10 samples were not as consistent and tended to break toward the top of the gage section. This appeared to be an artifact of the fixturing/machining process, as the #10 specimens were slightly thicker and wedge-shaped from end to end. Because of the uncertainty and data scatter among the #10 specimens, only the data for the #1, #4, and #7 specimens are reported here. The test results are summarized in Table 12.

Table 12: Summary of tensile test data.

Specimen ID	UTS, ksi	YS, ksi	% Elongation	RA, %
120-2U1	164.3	120.6	29.0	46.5
120-2U4	167.9	122.3	29.2	48.5
120-2U7	168.6	119.6	29.0	38.4
120-2L1	168.1	121.8	29.0	43.7
120-2L4	167.6	122.3	29.4	45.0
120-2L7	168.3	122.6	29.1	39.8
120°-2 Average	167.5	121.5	29.1	43.7
120-6U1	160.7	116.4	29.9	42.7
120-6U4	163.9	117.0	30.9	44.1
120-6U7	162.5	117.1	30.6	39.7
120-6L1	162.0	117.3	30.2	43.0
120-6L4	163.4	118.3	30.1	43.7
120-6L7	162.0	116.1	29.9	41.6
120°-6 Average	162.4	117.0	30.3	42.5
240-7U1	161.2	115.6	30.3	45.8
240-7U4	160.3	114.6	30.4	43.4
240-7U7	167.4	120.6	30.2	44.5
240-7L1	164.8	117.7	31.2	40.0
240-7L4	162.8	117.8	29.6	40.5
240-7L7	160.6	115.1	28.9	38.9
240°-7 Average	162.9	116.9	30.1	42.2
300-1U1	162.2	116.5	30.7	39.0
300-1U4	162.3	116.5	30.6	40.4
300-1U7	160.2	111.8	31.0	42.6
300-1L1	159.3	114.5	29.4	44.8
300-1L4	164.9	119.1	30.4	36.9
300-1L7	160.6	115.3	31.0	39.9
300°-1 Average	161.6	115.6	30.5	40.6